Paramagnetism and super paramagnetism of nanocrystalline titanium dioxide powders

E.K. Frolova [a,*], I.S. Petrik [b], O.Y. Kolomys [c], O.G. Sarbey [a], N.P. Smirnova [b], O.I. Oranska [c]

ARTICLE INFO

Keywords:
Magnetism
Nanoparticles
Titanium dioxide
Superparamagnetism
Oxygen vacancies

ABSTRACT

Studies of magnetization of undoped and Mn-doped nanosized titanium dioxide powders showed that its dependence on the magnetic field can be approximated by the function that is a linear combination of two Langevin functions with different parameters. The linear part along with the diamagnetic contribution typical for metal oxides is due to the contribution of two types of paramagnetic centers. The first one is present in both undoped and doped powders. As follows from the published models, the centers are complex lattice defects Ti^{+3} ions + O^{-} vacancies. The second is the vast majority of the manganese ions (and related oxide vacancies) in the doped powders that are uniformly distributed over all nanoparticles. The nonlinear part, even present in the undoped samples, is caused by the contribution of a small number of regions with a high magnetic moment (ferromagnetic clusters). These regions do not interact magnetically, and the powder as a whole exhibits superparamagnetic behavior. According to our estimates, the introduction of Mn into the TiO_2 lattice mainly leads to the predominance of the paramagnetic contribution to the magnetization over the diamagnetic contribution characteristic of the TiO_2 lattice and a small increase in the number of the ferromagnetic clusters.

1. Introduction

After ferromagnetism was detected at room temperature in thin TiO_2 films doped with Co [1] and in pure HfO_2 films [2], a lot of experimental [3-38] and theoretical [48-61] studies of this phenomenon were carried out in different materials. These are nanocrystalline powders [3-17] and thin films of metal oxides, pure and doped with magnetic ions [18-38].

The vast majority of these studies addressed the fundamental question of where the magnetic moment is localized in these unusual magnetic materials. In the case of TiO_2, various models of the magnetic center were proposed [8-24], but the following one is generally accepted at present. The local magnetic moment is associated either with the defective complex Ti^{+3} + O^{-} in pure titanium dioxide or with Ti^{+3} + Mn^{+2} + O^{-} in TiO_2 with Mn, and it is mainly distributed over three neighboring Ti atoms that are in immediate proximity to the oxygen vacancy.

A thorough analysis of all existing experimental data shows that the magnetizations in the region of ferromagnetic saturation of titanium dioxide in the form of nanofilms and nanopowders doped with Mn differ by 2–3 orders of magnitude (for example, data from works [10,19,26,29]). Accordingly, if we assume that all Mn ions participate in the ferromagnetic ordering, then the magnetic moment of the centers associated with them should differ by the same 2–3 orders of magnitude.

Although it cannot be argued that the magnetic moments associated with Mn in the films and powders should exactly match, such a big difference seems incredible.

However, this can be understood if we assume that in the vast majority of nanoparticles there is no spin ordering of magnetic moments (i.e., they are not ferromagnetic), and a very small part of them is involved in the appearance of ferromagnetism.

Thus, this work aimed to find out whether the directions of all magnetic moments of individual magnetic centers are correlated in each TiO_2 powder nanoparticle or only in some of them (or some set of nanoparticles).

We studied the magnetization of nanosized powders of both pure and Mn-doped titanium dioxide. To characterize the samples in which we observed ferromagnetism, we also measured X-ray diffraction and Raman spectra. This work is a continuation of the works published in [39,40], where some characteristics of such powders were obtained.

* Corresponding author.
E-mail address: frolova@iop.kiev.ua (E.K. Frolova).

https://doi.org/10.1016/j.jmmm.2021.167905
Received 3 July 2020; Accepted 25 February 2021
Available online 11 March 2021

2. Samples and experimental details

Titanium dioxide powders were synthesized by the sol–gel method using titanium isopropoxide as a precursor and a solution of C_2H_5OH/H_2O/HCl [39]. Manganese in the form of $MnCl_2{\cdot}4H_2O$ was introduced at the stage of the sol–gel process. Non-ionic amphiphilic triblock copolymer surfactant Pluronic (P123) and acetylacetone were used as a template and complex-forming agents. The syntheses were carried out at room temperature.

The obtained powders were dried and annealed at different temperatures up to 400 °C (for a more detailed description see [39,40]). It is known [44-49], that after such treatment the titanium dioxide already exists in the nanocrystalline form. Then, powders were successively annealed in the air for 3 h at temperatures of T_{an} = 400, 500, 600, and 650 °C, and after each stage of annealing, all measurements were performed at room temperature.

The concentration of Mn (defined as the ratio of the number of manganese ions and the sum of titanium and manganese ions) was determined from the weight ratio of the manganese and titanium compounds used for the synthesis. After synthesis, this ratio was not checked. Powders were synthesized with concentrations of Mn 0%, 1%, 2.9%, 4.7%, 6.5%, 9.1%, 16.6%, 23%.

XRD analysis of crystalline phases was carried out on a DRON-4–07 diffractometer (CuK_2 radiation with Ni filter) with Brag-Brentano registration geometry (2θ = 10–80°).

Raman spectra were obtained in quasi-backscattering geometry at room temperature using a 488-nm Ar/Kr laser line and a Horiba Jobin-Yvon T64000 triple spectrometer with an integrated micro-Raman scattering setup – an Olympus BX-41 microscope and a Peltier-cooled CCD detector. Magnetostatic measurements were carried out on an LDJ-9500 magnetometer with a vibrating sample. At the beginning of each measurement, the magnetic field rapidly increased to a maximum value of $+H_{max}$. Then the magnetic field decreased with a step of 10 G, passing through zero, and again increased in the opposite direction to $-H_{max}$. The magnetization was measured at each point. Then the measurements were repeated in the range from $-H_{max}$ through $+H_{max}$. We note that both curves obtained in this way are somewhat different from each other, especially at small field values. Due to the significant scatter of the measured points, we could not find the reason for this difference. All data below correspond to measurements with a change in the magnetic field from $-H_{max}$ to $+H_{max}$.

TiO_2 nanocrystals stick together, forming agglomerates of nanoparticles. TEM images show that these agglomerates have dimensions in the range of 0.2–0.5 μm. X-ray and Raman measurements were performed for all synthesized samples with an Mn concentration of 0–23%. Fig. 1 (as an example) shows X-ray diffraction patterns (a, c) and Raman spectra (b, d) of TiO_2 powders with Mn concentrations of 0–4.7% at various annealing temperatures. This choice is not accidental since in this concentration range the appearance of ferromagnetic regions is most pronounced. The X-ray diffraction studies show that these "large" formations contain a mixture of nanocrystals of two crystalline phases - anatase and rutile.

Some unstructured background at small diffraction angles (X-ray amorphous phase) is characteristic of nanocrystalline powders [3]. Line shape can be well described by the Voigt function. The position, width and integral intensity of the anatase lines 25.3^0 (101) and 48^0 (200) and rutile line 27.4^0 (110) were used to determine the composition of the mixture and the average size of nanocrystals. The composition (i.e.,

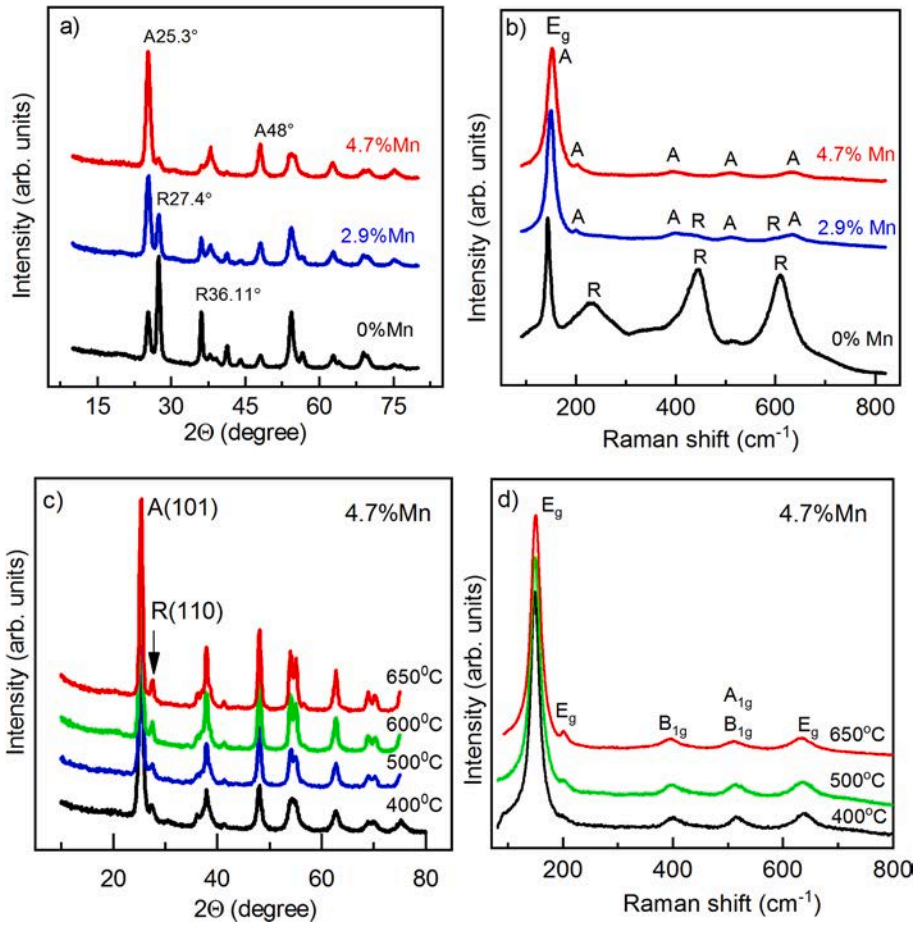

Fig 1. X-ray diffraction patterns (a, c) and Raman spectra (b, d) of TiO_2 powders with Mn: (a, b) – at various Mn concentrations after annealing at 400 °C; (c, d) – 4.7% Mn after annealing at different temperatures (with a zero offset along the Y-axis).

the rutile fraction in the anatase - rutile mixture) of the powder (W_R) was determined by the integral intensities of the anatase A_A (1 0 1) and rutile A_R (1 1 0) lines according to the Eq. (1) [42,43].

$$W_R = \frac{A_R}{0.886A_A + A_R} \quad (1)$$

Fig. 2 shows the dependence of W_R on the Mn concentration after annealing the powders at different temperatures.

It can be seen that the fraction of the rutile phase in the mixture decreases with increasing concentration of Mn. If it exceeds 6.5%, the rutile component cannot already be detected within the accuracy limits of the measurements (about 1% as estimated). Note that the rutile content is practically independent of the annealing temperature.

One should be emphasized that X-ray diffraction analysis shows that the presence of Mn in our samples does not lead to the appearance of new phases or compounds (at least, not more than 1%) [JCPDS file No. 21-1272]. It only changes the ratio of phases that exist in undoped TiO_2.

The average size of the nanocrystals was calculated by the Scherrer formula [41], assuming a spherical shape of particles without taking into account a possible contribution of defects to the line width.

Fig. 3 shows the dependence of this size on the Mn concentration for the anatase phase after annealing the powders at various temperatures.

First of all, it can be seen that the diameter of nanocrystals increases with increasing T_{an}, as expected. On the other side, the diameter tends to decrease when Mn concentration grows, at least at low concentrations of Mn. The presence of these two trends, probably, is the origin of irregularities in the dependence of the size of nanoparticles on the concentration of Mn at higher concentrations of manganese.

The size of nanocrystals in the rutile phase is larger (by 3–5 nm) than in the anatase phase, and depends on the Mn concentration, similarly to the anatase phase.

Given the size of the nanocrystals, their number per gram of the powder can be calculated. It varies from $5.6 \cdot 10^{16}$ to $6 \cdot 10^{17}$, depending on the temperature and manganese concentration.

Like X-ray spectra, all Raman spectra (one example is shown in Fig. 1 (b,d)) contain only lines characteristic of anatase and rutile. As in the X-ray spectrum, the rutile lines rapidly decrease in intensity with the introduction of Mn into TiO_2 powder.

The positions of the Raman peaks and their full width at half maximum (FWHM) are independent of the annealing temperature (at least within the spread of the points). However, the Raman shift and FWHM obtained by approximating the line shape by the Voigt function increase with increasing Mn concentration.

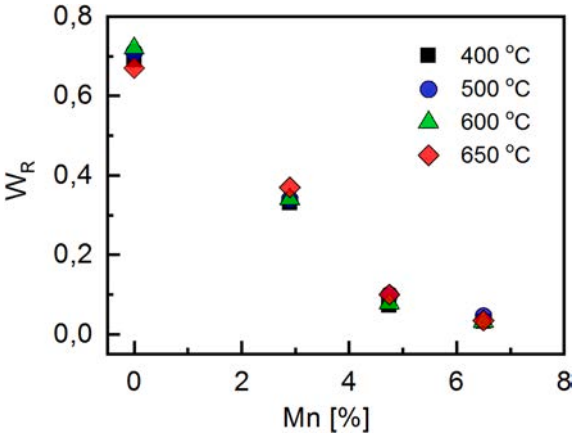

Fig 2. Dependence of composition of the powder mixture W_R on the concentration of Mn after annealing at different temperatures.

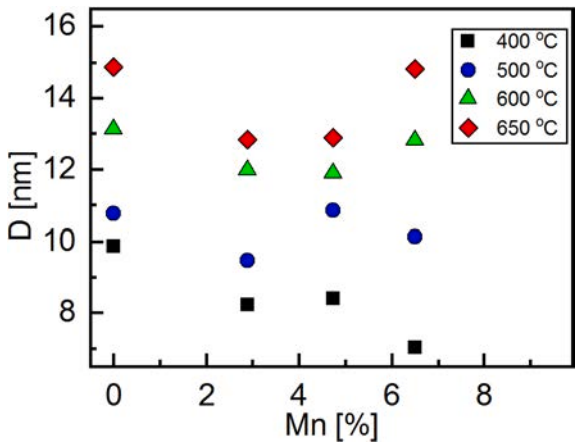

Fig 3. Dependence of the dimensions D of nanocrystals of the anatase phase on the concentration of Mn after different annealing temperatures.

3. Results of the magnetization measurements

Systematic measurements of the magnetization $M(H)$ of the TiO_2 powders were carried out for the samples with the Mn concentrations of 0, 2.9, 4.7, and 6.5%. Ferromagnetism is confidently observed in samples with such a concentration of Mn. Several measurements were made also for other concentrations. For example, Fig. 4 presents the dependencies of $M(H)$ for the undoped TiO_2 powder after annealing at 400 °C and 650 °C.

Both curves can be considered as a sum of two different curves. The first one is a straight line with a negative slope. It is most obviously expressed in the region of strong fields. This means that the powder in this region is mainly diamagnetic. The second one is a nonlinear curve with a positive curvature in the region of a weak field. The non-linear curve tends to saturate at the magnetic fields of the order of 2 to 2.5 kOe.

The $M(H)$ curves in the entire range of H are practically independent of the annealing temperature up to T_{an} = 650 °C. However, at T_{an} = 650 °C the nonlinear contribution in $M(H)$ at weak magnetic fields increases sharply while the linear diamagnetic contribution remains almost unchanged. When Mn is added into the TiO_2 powder, the linear component of the magnetization changes qualitatively. Its slope

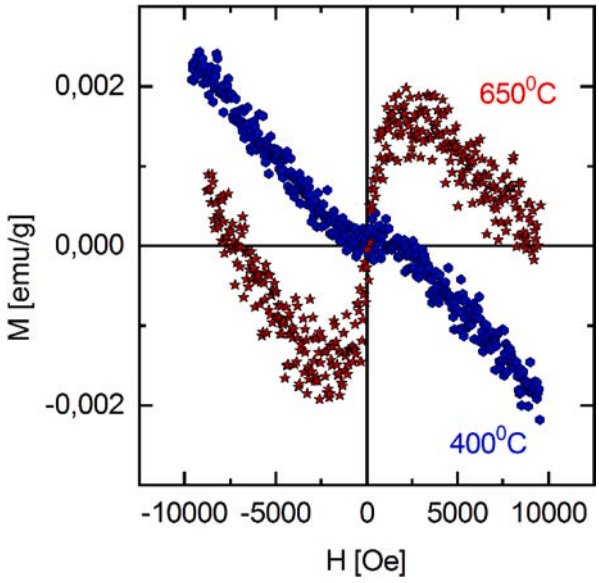

Fig 4. Dependences of magnetization on the magnetic field strength for the undoped powder after annealing at temperatures of 400 and 650 °C.

becomes positive (that is, the powder becomes paramagnetic, see Fig. 5 (a)), and the slope increases with increasing Mn concentration and is practically independent of the annealing temperature below 650 °C. However, the nonlinear component (as well as its value at saturation and the value of the magnetic field at the beginning of saturation) change insignificantly and unsystematically with the concentration of Mn and annealing temperature below 650 °C.

Annealing of powders at the temperature of 650 °C significantly affects the $M(H)$ curves. On average, the slope of the linear component at certain Mn concentrations decreases compared to its value at other temperatures, but the saturation of the nonlinear component sharply increases (as in the case of undoped TiO_2 powder). It should be noted that the magnetization values in the saturation region of the nonlinear component both for the undoped and doped powders fall into the range of published data [10,13,15,27,29,30].

Both components of magnetization can be described sufficiently well by the Langevin function $L(x)$ (see Fig. 5(a) and 5(b))

$$L(x) \approx coth(x) - \frac{1}{x} \tag{2}$$

We use its expansion for $|x| < 1$ in the case of the linear component

$$L(x) \approx \mathrm{CH} = \frac{x}{3} \tag{3}$$

and the whole function (expression (2)) for the nonlinear one. The argument x in $L(x)$ is connected with the value of the magnetic moment m of the magnetic centers, which differs for the linear m_l and nonlinear m_n components of magnetization

$$x = \frac{mH}{kT} \tag{4}$$

where T is the temperature of measurements, k is the Boltzmann constant. The linear and nonlinear components of magnetization are given by

$$M_{l,n}(H) = m_{l,n} N_{l,n} L(x) \tag{5}$$

were $N_{l,n}$ is the concentration of magnetic moments $m_{l,n}$.

Hereinafter, all quantities of $M_{l,n}(H)$, $N_{l,n}$, the number of nanoparticles, magnetic moments, etc. refer to one gram of a substance.

Fig. 6(a) shows the dependence of the linear part of the magnetic susceptibility χ_l on the Mn concentration obtained by fitting the measured data using the sum of the expressions (2) and (3):

$$M = m_n N_n \left[\coth\left(\frac{m_n H}{kT}\right) - \frac{kT}{m_n H} \right] + \chi_l H, \text{ where } \chi_l = \frac{m_l^2 N_l}{3kT} \tag{6}$$

Despite the scatter of χ_l values and without taking into account peculiarities in the range between 5 and 10% of Mn (the possible origin of the irregularities will be discussed below) it can be approximated by a straight line for all annealing temperatures. By the aforesaid, these lines practically coincide with the annealing temperatures of 400, 500, and 600 °C, but the line for 650 °C has a smaller slope.

One point should be made about Fig. 6(a). We associate the diamagnetism in the undoped titanium dioxide with the TiO_2 lattice (see discussion later). In samples doped with Mn, it is not visible against the background of the larger paramagnetic component. We reckon that this diamagnetism should be present in the measured magnetization in all of our powders. Therefore, for a correct assessment of the paramagnetic component caused by doping of TiO_2 with Mn ions, it should be subtracted from the total measured magnetization. The data obtained precisely by this way for the linear paramagnetic component of the magnetic susceptibility are depicted in Fig. 6(a).

The dependences of the magnetic moment m_n of the regions with correlated magnetic moments and their concentration N_n (the nonlinear magnetization component) on the Mn concentration after annealing at the temperatures of 400, 500 and 650 °C are presented in Fig. 7(a) and (b), respectively.

It should be noted that we determine these values with relatively low accuracy (~30%). Therefore, it cannot be unambiguously concluded that they depend on the Mn concentration and the annealing temperature. In general, a significant increase in N_n is observed only for the powder with the Mn concentration of 4.7% after annealing at a temperature of 650 °C.

The values of m_n and N_n for the nonlinear magnetization component were calculated using relationship (6) to fit the measured points $M(H)$. The results are given in Table 1.

4. Discussion

In an overwhelming majority of papers, it is assumed that ferromagnetism at room temperature, both in the doped and "pure" metal oxides, is connected anyhow with the presence of the oxide vacancies (V_O). The experiments with cyclic annealing of TiO_2 films or powders in a vacuum (or in the hydrogen flux) and then in air confirm this fact. Indeed, when the samples are annealed in a vacuum and the vacancies concentration is increased, the magnitude of the magnetization saturation in the nonlinear region increases sharply [6,9]. Conversely, it decreases or even disappears completely after annealing samples in air or the oxygen ambient [9]. According to these experiments, there is no doubt that the presence of the oxide vacancies is necessary to form a

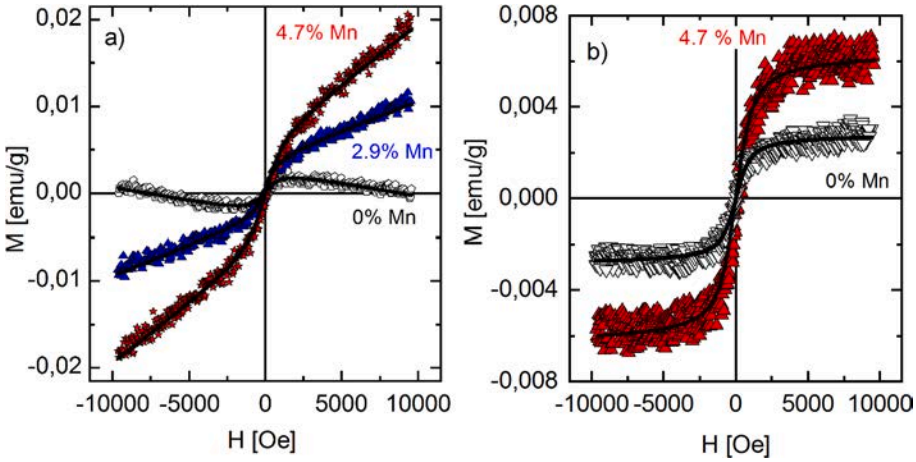

Fig 5. Magnetization dependences on magnetic field H for the undoped and doped TiO_2 after annealing at 650 °C: (a) measurement results; (b) the nonlinear component of $M(H)$ after excluding the linear component from data in Fig. 5(a) (point-experiment, solid line - approximation using relationship (6) to fit the experimental of M (H).

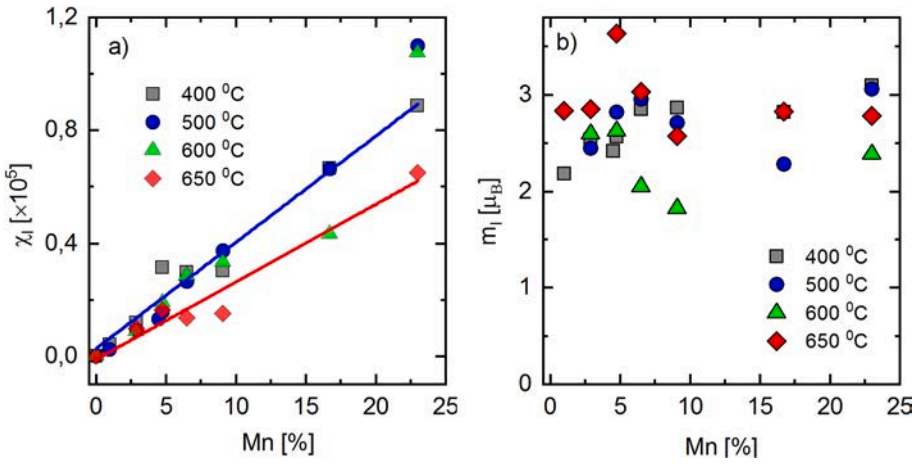

Fig 6. Dependence of the magnetic susceptibility χ_l (a) and magnetic moment m_l of manganese ions (b) on the concentration of Mn for the linear component $M(H)$.

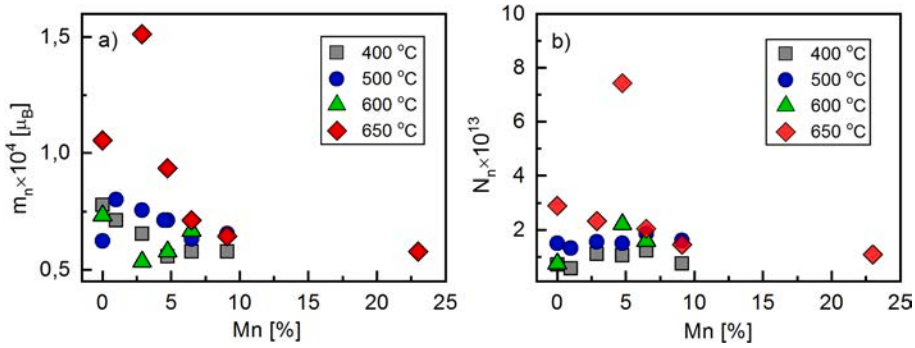

Fig 7. The dependencies of m_n(a) and N_n (b) on the Mn concentration after annealing at temperatures 400, 500, 600, and 650 °C.

Table 1
The results of the approximation of the experimental curves $M(H)$ using dependence (6) for 400 °C and 650 °C where Mn % is the Mn concentration, N_{Mn} is the amount of Mn ions, N_{np} is the number of nanoparticles per gram of powder, m_n and N_n are the magnetic moments and the number of ferromagnetically ordered regions, respectively.

		T = 400 °C			T = 650 °C		
Mn %	$N_{Mn}\times 10^{20}$ [g^{-1}]	$N_{np}\times 10^{17}$ [g^{-1}]	$m_n\times 10^4$ [μ_B]	$N_n\times 10^{13}$ [g^{-1}]	$N_{np}\times 10^{17}$ [g^{-1}]	$m_n\times 10^4$ [μ_B]	$N_n\times 10^{13}$ [g^{-1}]
0	0	5.2	0.78	0.72	1.5	1.0	2.9
2.9	2.1	8.9	0.65	1.1	2.3	1.3	2.4
4.7	3.4	6.7	0.56	1.0	2.3	0.93	7.4
6.5	4.6	14	0.58	1.2	1.5	0.81	2.0

local magnetic moment and collective magnetism.

Although there are different models for a specific role of the oxide vacancies [6-26], the following one is now generally accepted. The local magnetic moment in the undoped films and bulk powders is associated with the defect $Ti^{+3} + O^-$ complex and the magnetic moment is mainly distributed over three neighboring atoms of Ti closest to V_O. Below we use the term "magnetic moment of vacancy" only in this respect, for simplicity.

As follows from the literature [7,8,16,19,31], Mn ions in the TiO_2 lattice replaces tetravalent titanium ions mainly in the form of divalent ions. For our powders, this is confirmed by measurements of the XPS spectra published previously by some co-authors [39].

To maintain charge neutrality, upon the introduction of the divalent Mn ion at the site of the tetravalent Ti ion, an oxygen vacancy appears at the site of the oxygen atom closest to the Mn ion. It means that these vacancies appear additionally in the volume of the nanoparticle.

Our Raman spectra confirm this. As shown in [62], the introduction of impurities of foreign atoms into the TiO_2 lattice does not change the Raman spectrum, but the introduction of oxygen vacancies causes the shift and broadening of some spectral lines.

Fig. 8 shows the dependence of the position of the most intense Raman peak of anatase (E_g) on the concentration of Mn measured in this work (points on the graph correspond to different annealing temperatures of powders). The solid line in this figure is the calibration curve of the dependence of the position of the same peak on the concentration of oxygen vacancies, which we obtained using relevant data from [62].

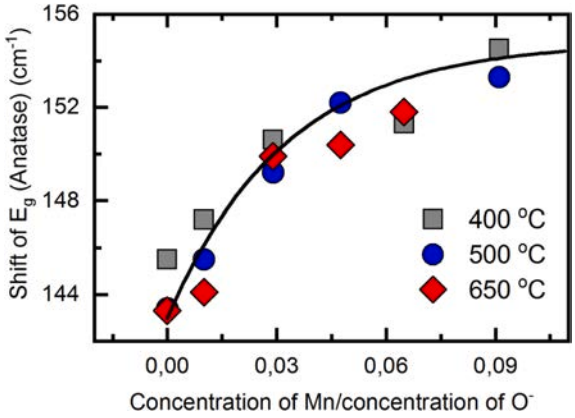

Fig 8. The dependencies of Raman shift E_g anatase line on the Mn concentration (symbols - our results) and the O^- concentration (curve - restored according to the results of [71]).

It can be seen that our measured peak positions satisfactorily correspond to the calibration curve. This means that the concentrations of Mn ions and oxygen vacancies are equal, i.e., the introduction of each Mn ion is indeed accompanied by the appearance of an oxygen vacancy.

The bulk TiO_2 is diamagnetic with magnetic susceptibility about -10^{-6} g^{-1} [24]. However, the magnetic susceptibility of our undoped TiO_2 powder is by about 3 times less. We associate this difference with the presence of a large amount of the oxide vacancies in the powder grains and their paramagnetism, which partially compensates for the diamagnetism of the TiO_2 lattice. If this is the case, then the concentration of vacancies in our powders should be about $2.5 \cdot 10^{20}$ g^{-1}. For this estimate, we used the magnetic moment of the vacancy for undoped TiO_2 equal to $2\mu_B$, as calculated in [49,57].

At first glance, this value contradicts the data given in Fig. 8, according to which the concentration of vacancies in our undoped TiO_2 powder is close to zero. Indeed, due to the high formation energy (4.2–4.4 eV) [49,50], in a volume of pure TiO_2 the equilibrium concentration of vacancies inside nanoparticles should be negligible. Oxygen vacancies, however, can be present near the surface of nanoparticles where formation energy has to be essentially smaller. These vacancies are distributed more or less evenly near the surface of all nanoparticles; they cannot be detected in our Raman measurements.

We believe that the magnetic moments associated with these vacancies do not interact with each other for most particles and cause the paramagnetic component of magnetization in pure TiO_2. Introducing the Mn^{2+} ions into TiO_2 in the process of the sample synthesis, we cannot properly take into account the contribution of these near-surface vacancies to paramagnetism. Their different contributions in different powders can be the reason for the scatter of the measured points and irregularities in the dependence of χ_l on the concentration of the Mn ions, as mentioned above (Fig. 6(a)).

Nevertheless, there are areas in the powders where the concentration of the oxide vacancies and their amount can be large enough to cause collective magnetism. These could be, for example, near-surface regions of relatively large nanoparticles or contact regions between nanoparticles (including nanoparticles of different phases).

We estimated the total number of vacancies in such regions in pure TiO_2 using both the maximal value of the saturation magnetization for the nonlinear component (~0.003 emu/g for $T_{an} = 650$ °C) the value of the magnetic moment of the vacancy $2\mu_B$, given above, as $2.7 \cdot 10^{17} g^{-1}$.

A similar estimate for the Mn-doped TiO_2 (even if we assume that all the magnetization in saturation is due to the magnetic moment connected with Mn, and not to "native" vacancies of the undoped TiO_2 and Mn together) gives the value $6.9 \cdot 10^{17} g^{-1}$.

This value is much less than the amount of the Mn ions included in TiO_2 (column 2 in Table 1). Therefore, we assume that the amount of the Mn ions responsible for the linear part of sample magnetization to be practically equal to the amount of the Mn atoms introduced into the TiO_2 matrix. Consequently, according to the data in Fig. 6(a), it is possible to determine the local magnetic moment associated with the Mn ions. The results are shown in Fig. 6(b). As can be seen, the average magnetic moment is about 2.4 μ_B for Tan = 650 °C and 2.9 μ_B for the other annealing temperatures. These values do not contradict the data obtained in experiments with the TiO_2 films doped by Mn [7,17,23,29,38]. The value of 2.9 μ_B is also consistent with the theoretically calculated value of 3.4 μ_B [30].

The effective magnetic moment m_n responsible for the nonlinear component of magnetization in both undoped and doped samples is much larger than in the linear region and has a value of about $10^4 \mu_B$.

Such a large value gives evidence for the magnetic moment to be connected with areas of correlated behavior (magnetic ordering) of a large number of local moments, as mentioned above. The number of these N_n regions is close to 10^{13} g^{-1}, being several orders of magnitude less as compared to the number of nanoparticles (columns 3 and 6 in Table 1). Thus, most nanoparticles are not ferromagnetic, but rather paramagnetic. They contribute only to the linear component of magnetization. And only a very small part of them is about 10^{-4}, has a pronounced ferromagnetic ordering and is responsible for the nonlinear part of $M(H)$. The magnetic moments of these magneto-ordered regions do not interact with each other. In the magnetic field their ensemble does not behave as a ferromagnetic material, but rather as a superparamagnetic one with the magnetization saturation at relatively weak fields and without a pronounced hysteresis loop.

As follows from the data presented in Fig. 7 and Table 1, the nonlinear component of the TiO_2 magnetization is almost not affected by the introduction of Mn into the TiO_2 matrix. A clearly pronounced increase in the value of saturation magnetization occurs only at relatively high concentrations of Mn (3–5%). At first glance, this result is unexpected. However, we have to keep in mind that the magnetic moment and concentration of "native" vacancies in our samples of the undoped TiO_2 are comparable to the magnetic moment and concentration of the Mn ions. Consequently, the replacement of the Ti ion with Mn ion in the magnetically ordered region does not significantly change its effective magnetic moment m_n.

We would like to point out that the saturation values of magnetization in the nonlinear region $M(H)$ in our experiments are of the order of 10^{-3}–10^{-2} emu g^{-1}. It coincides more or less (recall that our samples were annealed in the air) with the previously published data both for the doped and undoped powders [4,6,10,13,15,25,27,29].

Finally, we would like to discuss briefly the question of why the vast majority of nanoparticles in our measurements do not exhibit ferromagnetism. We assume that for small particles a decisive role play conditions on the surface of the nanoparticle. First of all, we note that, for example, for a ball-shaped nanoparticle about 10 nm in size, the volume of the surface layer (with a thickness of the constant "a" of the TiO_2 unit cell) takes about 10% of its total volume. Most of the oxygen vacancies with which the magnetic moment is associated are located in this layer.

If the particles are not flat, the surface area vector changes its direction at small distances along the surface. Thus, there is no well-defined one direction for the spin ordering of magnetic moments, and therefore a single nanoparticle cannot possess ferromagnetism.

In this regard, nanoparticles are fundamentally different from nanofilms, where the surface is flat and there is at least one distinguished direction on the entire surface.

5. Conclusion

We found that the manganese ions included in the TiO_2 powder do not lead to the appearance of ferromagnetism as a common phenomenon for all nanoparticles of the powder. The manganese ions are substantially homogeneously distributed in the bulk of all sample particles and provide the paramagnetic contribution into the magnetization of the powder with the magnetic susceptibility proportional to the Mn concentration. On the other hand, the sample contains a small number of regions with the ferromagnetic ordering of the unpaired spins, which do not interact with each other, and their ensemble in the magnetic field behaves like superparamagnetic. Such regions appear in the samples both doped and undoped with the Mn ions. The presence of manganese ions increases the number of such regions but not changes their magnetic moment essentially.

Declaration of Competing Interest

The authors declare that they have no known competing financial interests or personal relationships that could have appeared to influence the work reported in this paper.

Acknowledgment

The authors are pleased to thank Professor S.M. Ryabchenko for helpful discussions and professional advice. Our gratitude to Dr. N.N.

Kulik for help in conducting magnetic measurements and V.I. Styopkin who determined for us the size of the TiO_2 nanoparticles agglomerates using the electron microscopy.

References

[1] Y. Matsumoto, M. Murakami, T. Shono, T. Hasegawa, T. Fukumura, M. Kawasaki, P. Ahmet, T. Chikyow, S. Koshihara, H. Koinuma, Science 291 (2001) 854.
[2] M. Venkatesan, C.B. Fitzgerald, J.M.D. Coey, Nature 430 (2004) 630.
[3] A. Sundaresan, R. Bhargavi, N. Rangarajan, U. Siddesh, and C.N.R. Rao, Phys. Rev. B 74, 161306(R) (2006); A. Sundaresan, C.N.R. Rao, Nano Today 4, 96 (2009).
[4] S. Banerjee, M. Mandal, N. Gayathriand M. Sardar, Appl. Phys. Lett. 91, 182501 (2007).
[5] K. Ghosh, P.K. Kahol, S. Bhamidipati, N. Das, S. Khanra, A. Wanekaya, R. Delong, AIP Conf. Proc. 1461 (2012) 87.
[6] S. Sharma, S. Chaudhary, S.C. Kashyap, J. Supercond. Novel Magn. 24 (2011) 839.
[7] Z.V. Saponjic, N.M. Dimitrijevic, O.G. Poluektov, L.X. Chen, E. Wasinger, Ulrich Welp, D.M. Tiede, X. Zuo, T. Rajh, J. Phys. Chem. B 110 (2006) 25441.
[8] S. Bhattacharyya, A. Pucci, D. Zitoun, A. Gedanken, Nanotechnology 19 (2008), 495711.
[9] B. Choudhury, A. Choudhury, J. Appl. Phys. 114, 203906 (2013); B. Choudhury, R. Verma, A. Choudhury, RSC Adv. 4, 29314 (2014).
[10] L. Zhang, L. Zhu, L. Hu, Y. Li, H. Song, Z. Ye, RSC Adv. 6 (2016) 57403.
[11] S. Zhou (周生强), E. Cizmar, K. Potzger, M. Krause, G. Talut, M. Helm, J. Fassbender, S. A. Zvyagin, J. Wosnitza, H. Schmidt, Phys. Rev. B 79, 113201 (2009) .
[12] R.K. Singhal, Sudhish Kumar, P. Kumari, Y.T. Xing, and E. Saitovitch, Appl. Phys. Lett. 98, 092510 (2011).
[13] N.N. Hai, N. Khoi, P. VanVinh, J. Phys. Conf. Series 187 (2009), 012071.
[14] B. Santara, P.K. Giri, K. Imakita, M. Fujii, Nanoscale 5 (2013) 5476.
[15] A.E. Ermakov, M.A. Uimin, A.V. Korolev, A.S. Volegov, I.V. Byzov, N. N. Shchegoleva, A.S. Minin, Phys. Solid State 59 (2017) 469.
[16] D. Menzel, I. Jursic, J. Schoenes, D. Cacaina, Phys. Status Solidi C 3 (2006) 4119.
[17] C. Das Pemmaraju, S. Sanvito, Phys. Rev. Lett. 94 (2005), 217205.
[18] J. Antony, Y. Qiang, M. Faheem, D. Meyer, Appl. Phys. Lett. 90 (2007), 013106.
[19] S. Sharma, S. Chaudhary, S.C. Kashyap, S.K. Sharma, J. Appl. Phys. 109 (2011), 083905.
[20] X. Li, S. Wu, P. Hu, X. Xing, Y. Liu, Y.Yu. Yang, J. Lu, S. Li, W. Liu, J. Appl. Phys. 106 (2009), 043913.
[21] X.Y. Li, S.X. Wu, L.M. Xu, Y.J. Liu, X.J. Xing, S.W. Li, J. Appl. Phys. 104 (2008), 093914.
[22] X.Y. Li, J.R. Xiao, Z.Y. Wang, S.W. Li, J. Mater. Sci. Eng. B 177 (2012) 869.
[23] J.P. Xu, Y.B. Lin, Z.H. Lu, X.C. Liu, Z.L. Lu, J.F. Wang, W.Q. Zou, L.Y. Lv, F.M. Zhang_, Y.W. Du, Solid State Commun. 140, 514 (2006).
[24] MLF[24] J. Tian, H. Gao, H. Kong, P. Yang, W. Zhang, J. Chu, Nanoscale Res. Lett. 8, 533 (2013).
[25] O. Yıldırım, S. Cornelius, M. Butterling, W. Anwand, A. Wagner, A. Steklova, J. Fiedler, R. Bottger, C. Bahtz, K. Potzger, Appl. Phys. Lett. 107 (2015), 242405.
[26] N.H. Hong, J. Sakai, N. Poirot, V. Brize, Phys. Rev. B 73 (2006), 132404.
[27] G.H. Lee, J.M. Zuo, J. Am. Ceram. Soc. 87 (2004) 473.
[28] K. Ueda, H. Tabata, T. Kawai, Appl. Phys. Lett. 79 (2001) 988.
[29] J.P. Xu, J.F. Wang, Y.B. Lin, X.C. Liu, Z.L. Lu, Z.H. Lu, L.Y. Lv, F.M. Zhang, Y. W. Du, J. Phys. D: Appl. Phys. 40 (2007) 4757.
[30] Z. Zhou, X. Yang, H. Wang, Z. Zou, J. Guo, Adv. Condens. Matter Phys. ID 1562596 (2016) 7.
[31] FM[31] S. Kumar, S. Gautam, G.W. Kim, Faheem Ahmed,.M.S. Anwar, K.H. Chae, H.K. Choi, H. Chung, B.H. Koo, Appl. Surf. Sci. 257,10557 (2011).
[32] J.Y. Yang, Y.L. Han, L. He, R.F. Dou, C.M. Xiong, J.C. Nie, Appl. Phys. Lett. 100 (2012), 202409.
[33] X. Li, S.Wu, P.Hu, X. Xing, Y. Liu, Y. Yu, M.i Yang, J. Lu, S. Li, W. Liu, J.Appl. Phys. 106, 043913 (2009).
[34] Y. Yamada, K. Ueno, T. Fukumura, H.T. Yuan, H. Shimotani, Y. Iwasa, L. Gu, S. Tsukimoto, Y. Ikuhara, M. Kawasaki, Science 332 (2011) 1065.
[35] H.J. Meng, D.L. Hou, L.Y. Jia, X.J. Ye, H.J. Zhou, X.L. Li, J. Appl. Phys. 102 (2007), 073905.
[36] O. Yildirim, S. Cornelius, A. Smekhova, G. Zykov, E.A. Gan'shina, A.B. Granovsky, R. H€ubner, C. B€ahtz, K. Potzger, J. Appl. Phys. 117, 183901 (2015).
[37] M.C.K. Sellers, E.G. Seebauer, Appl. Phys. A 104 (2011) 583.
[38] J.P. Xu, S.B. Shi, L. Li, J.F. Wang, L.Y. Lv, F.M. Zhang, Y.W. Du, J. Phys. Chem. Solids 70, 511 (2009).
[39] I.S. Petrik, G.V. Krylova, O.O. Kelyp, L.V. Lutsenko, N.P. Smirnova, L.P. Oleksenko, CPTS 2015. V. 6. N 2. (Chemistry, Physics, and Technology of Surface. 2015. V. 6. N 2. P. 179-189).
[40] N. Smirnova, I. Petrik, V. Vorobets, G. Kolbasov, A. Eremenko, Nanoscale Res. Lett. 12 (2017) 239.
[41] A.L. Patterson, Phys. Rev. 56 (1939) 15.
[42] R.A. Spurr, H. Myers, Anal. Chem. 29 (5) (1957) 760.
[43] Amy A. Gribb, Jillian F. Banfield, Am. Mineral. 82 (1997) 717.
[44] H. Zhang, J.F. Banfield, J. Mater. Chem. 8 (9) (1998) 2073.
[45] H. Zhang, J.F. Banfield, J. Phys. Chem. B 104 (2000) 3481.
[46] W. Li, C. Ni, H. Lin, C.P. Huang, S. Ismat Shah, J. Appl. Phys. 96 (2004) 6663.
[47] N. Satoh, T. Nakashima, K. Yamamoto, Sci. Rep. 3 (2013) 1959.
[48] K. Kenmochi, M. Seike, K. Sato, A. Yanase, H. Katayama-Yoshida, Jpn. J. Appl. Phys. 43 (2004) L934.
[49] Guang-bing Han, Shu-jun Hu, Shi-shen Yan, and Liang-mo Mei, Phys. Status Solidi RRL3, 148 (2009).
[50] C. Di Valentin, G. Pacchioni, A. Selloni, Chem. Mater. 17 (2005) 6656.
[51] H. Wang, Z. Zong, Yu. Yan, J. Appl. Phys. 115 (2014), 233909.
[52] D. Kim, J. Hong, Y.R. Park, K.J. Kim, J. Phys.: Condens. Matter 21 (2009), 195405.
[53] I.S. Elfimov, S. Yunoki, G.A. Sawatzky, Phys. Rev. Lett. 89 (2002), 216403.
[54] Q. Wang, Q. Sun, G. Chen, Y. Kawazoe, P. Jena, Phys. Rev. B 77 (2008), 205411.
[55] G. Rahman, V.M. García-Suárez, S.C. Hong, Phys. Rev. B 78 (2008), 184404.
[56] H.W. Peng, J.B. Li, S.S. Li, J.B. Xia, Phys. Rev. B 79 (2009), 092411.
[57] P.J.D. Lindan, N.M. Harrison, M.J. Gillan, J.A. White, Phys. Rev. B 55 (1997) 15919.
[58] D.Q. Fang, R.Q. Zhang, J. Appl. Phys. 109 (2011), 044306.
[59] I. Justicia, P. Ordejon, G. Canto, J.L. Mozos, J. Fraxedas, G.A. Battiston, R. Gerbasi, A. Figueras, Adv. Mater. 14 (2002) 1399.
[60] J.M.D. Coey, M. Venkatesan, P. Stamenov, C.B. Fitzgerald, L.S. Dorneles, Phys. Rev. B 72 (2005), 024450.
[61] V.G. Zavodinsky, A.N. Chibisov, Physics of Solid State (ru) 51 (2009) 507.
[62] J. C. Parker and R.W. Siegel, J. Mater. Res., Vol. 5, No. 6, Jun 1990; Appl. Phys. Lett. 51 (9), 1990; Acta Metallurgica Conference on "Materials with Ultrafine Microstructures ", Atlantic City, New Jersey, October 1-5, 1990.